NJC

Accepted Manuscript

This article can be cited before page numbers have been issued, to do this please use: D. Ramaiah, S. THURAKKAL, K. S. Sanju, A. Soman, N. Unni and J. Joseph, *New J. Chem.*, 2018, DOI: 10.1039/C7NJ04386D.

ROYAL SOCIETY OF CHEMISTRY

rsc.li/njc

View Article Online
DOI: 10.1039/C7NJ04386D

Journal Name

ARTICLE

Design and synthesis of solution processable green fluorescent D-π-A dyads for OLED applications

Received 00th January 20xx,
Accepted 00th January 20xx

DOI: 10.1039/x0xx00000x

www.rsc.org/

Shameel Thurakkal,[a,b] Krishnankutty S. Sanju,[a,c] Anjaly Soman,[a,b] K. N. Narayanan Unni,[a,b] Joshy Joseph,[a,b] and Danaboyina Ramaiah [a,d]

New solution processable organic donor-π-acceptor dyads **1** and **2** having electron donating phenoxazine and accepting oxadiazole groups have been synthesized. Intramolecular electron communication between the donor and acceptor moieties of these dyads was tuned through changing the substitution pattern at the phenylene linker. The photophysical properties of these dyads have been studied in the solution and film states. These dyads showed green fluorescence and exhibited a positive solvatochromism in the emission spectra which indicates more polar excited states owing to an efficient charge migration from the donor phenoxazine to the acceptor oxadiazole moiety. The electrochemical, morphological and thermal properties were investigated through cyclic voltammetry, thermogravimetric and atomic force microscopy (AFM) analyses. To understand the electronic structure and band gap of these dyads, density functional theory (DFT) calculations have been performed. Furthermore, we have fabricated the solution processed un-doped electroluminescence devices based on these dyads, which exhibited efficient green emission with Commission Internationale de l'E´clairage (CIE) coordinates of (0.26, 0.49) and (0.27, 0.47) for **1** and **2**, respectively, with a luminance maximum of ca.1751 cd/m^2 for the dyad **1**, thereby demonstrating its use in organic light emitting diodes (OLED$_S$).

Introduction

Organic light emitting diodes are considered as the most desirable device architectures for the next generation flat panel displays and solid state lightning devices.[1] In this context, design of novel organic luminescent molecules for OLEDs and study of their structure-property relationship have attracted much attention since the pioneering work of Tang and Vanslyke in 1980s.[2] New emitting materials for the development of efficient devices is quite challenging in this field and also understanding the interactions and solid state properties due to substitution have great importance as this would help in improving the device efficiency.[3]

The fluorescent and phosphorescent OLEDs of multilayered structures with host dopant systems have been widely reported.[4] Typically, in a multilayer device, various layers, such as hole transport layer, emitting layer and electron transport layer, were deposited in between the anode and cathode.[5] Considering the practical applications, sequential layer-by-layer fabrication procedures and the precise control of host-dopant ratio increases the complexity and thus the cost of such OLEDs.[6] For this reason, the organic light emitting materials possessing electron and hole transporting characteristics, called bipolar molecules are being developed, such that the device can be simplified to double or single layer device architecture.[7] The bipolar charge transport can be achieved by incorporating both electron donating and withdrawing moieties into the same molecule.[8] Further, these unsymmetrical structures, when substituted with long alkyl chains provide better solubility and thereby their improved solution processability and reduced aggregation induced quenching (ACQ) of emission intensity.[9]

Among the various fluorophores, the green emitters have a great deal of importance since it is one of the three primary colors used for the white light emission.[10] The small organic donor-acceptor type fluorophores have distinct advantages in OLED fabrication over polymers and inorganic compounds. These include their comparatively simple synthesis, purification and analysis.[11] In addition, donor-acceptor structure can have large degree of control over the electronic

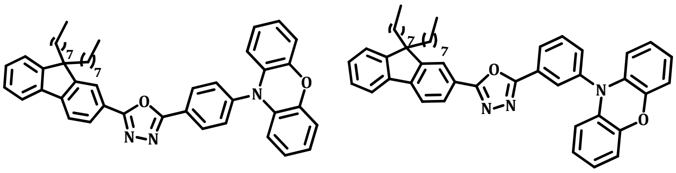

1 2

Chart 1 Structures of the donor-acceptor dyads **1** and **2** investigated

---

[a] Photosciences and Photonics, Chemical Sciences and Technology Division,CSIR-National Institute for Interdisciplinary Science and Technology, Thiruvananthapuram-695019, Kerala, India.

[b] Academy of Scientific and Innovative Research (AcSIR), CSIR-NIIST Campus, Thiruvananthapuram-695019, Kerala, India.

[c] CSIR- Central Institute of Mining and Fuel Research, Dhanbad-826015, Jharkhand, India.

[d] CSIR-North East Institute of Science and Technology, Jorhat-785006, Assam, India. E-mail: rama@neist.res.in, d.ramaiah@gmail.com

†Electronic Supplementary Information (ESI) available: Fig. S1–S15 and Tables S1–S2 show the characterisation, photophysical, computational and device data of the dyads. See DOI: 10.1039/x0xx00000x

View Article Online
DOI: 10.1039/C7NJ04386D

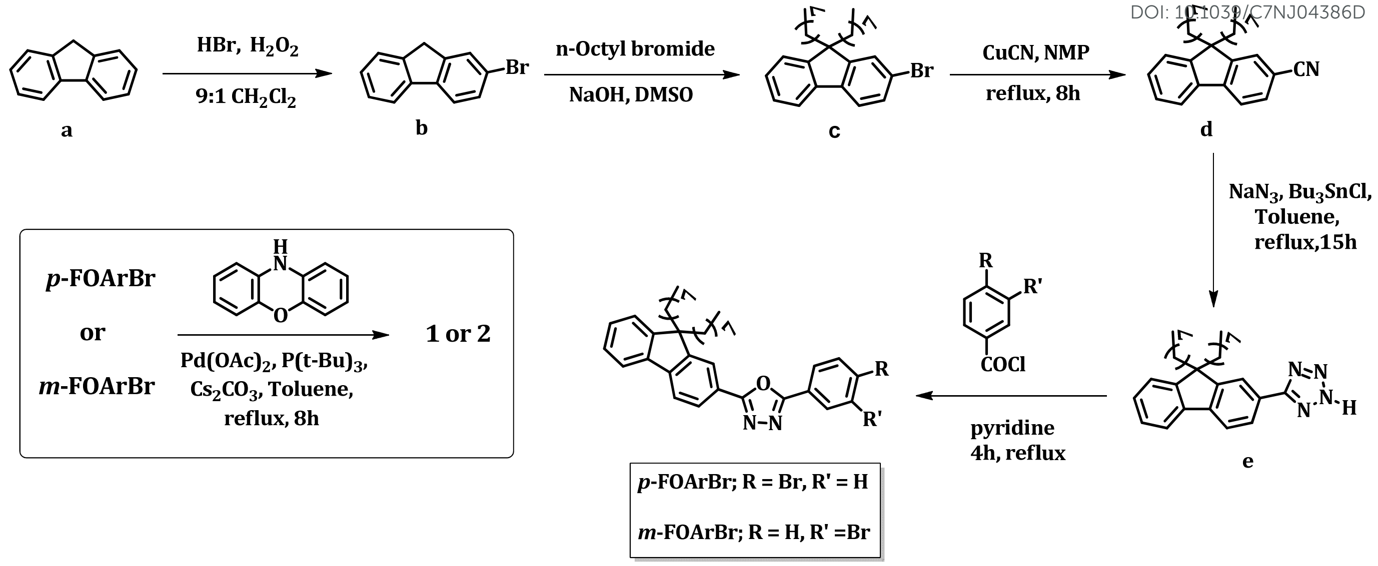

Scheme 1 Synthetic method adopted for the donor-acceptor dyads **1** and **2**.

and optical properties in accordance with their structural modification.[12] In this respect, the development of non-doped OLEDs based on solution processable small molecules with bipolar characteristics are highly desirable for their commercialization. In general, the materials having electron withdrawing molecular building blocks like oxadiazoles, pyridine, phenanthroline, benzimidazole, quinolines, triazines, and quinoxalines have been used as electron transport building blocks in OLEDs.[13-19] Among these, 1,3,4-oxadiazoles are well-known for their electron transporting and hole blocking abilities due to their electron deficient nature.[20] Moreover, incorporation of such oxadiazole group found to enhance the thermal stability, which is an essential property of OLED materials.[21] On the other hand, the electron donating building blocks like carbazoles,[22] diphenylamine,[23] phenoxazine,[24] and phenothiazine,[25] were extensively studied. The phenoxazine derivatives have been widely used in the design of green emitters and as hole transporting materials.[26] Herein, we report the luminescent dyads **1** and **2** (Chart 1) having electron donating phenoxazine and accepting oxadiazole moieties and investigation of their photophysical, morphological aspects and also their use in OLEDs. Interestingly, these systems exhibited substitution dependent photophysical properties and as green emitters in the device performance wherein we observed the maximum luminescence intensity of ca.1751 cd/m^2 for the dyad **1**, thereby indicating its potential use in OLEDs applications.

Results and discussion

Design and synthesis of donor acceptor system

The designed molecules have donor phenoxazine and acceptor 2-(9,9-dioctyl-9H-fluoren-2-yl)-1,3,4-oxadiazole linked through a phenylene linker by para- (dyad **1**) and meta- (dyad **2**) substitution. To achieve the solution processability, we have adopted the unsymmetrical structures, incorporating long alkyl chains. The precursors, *p*-FOArBr and *m*-FOArBr were synthesized by modifying the reported procedures, in ca. 69-75% yields (Scheme 1).[27] The mono bromination of fluorene followed by the alkylation yielded 2-bromo-9,9-dioctyl-9H-fluorene in good yields. The product upon Rosenmund-von Braun reaction gave the corresponding carbonitrile derivatives, 9,9-dioctyl-9H-fluorene-2-carbonitrile in *ca.* 60-70% yields. The tetrazole derivatives, on the other hand, were prepared and which on refluxing with para- and meta- bromobenzoyl chlorides gave the precursors *p*-FOArBr and *m*-FOArBr in excellent yields.

The synthesis of the target molecules was achieved through Buchwald-Hartwig coupling reaction between donor and acceptor molecules.[28] The phenoxazine system upon Pd-catalyzed cross-coupling reaction with *p*-FOArBr and *m*-FOArBr in presence of cesium carbonate as the additive base, gave the conjugates **1** and **2** in *ca.* 80 and 75% yields, respectively. The starting materials as well as the dyads were purified through column chromatography and recrystallization and were characterized on the basis of spectroscopic and analytical evidence (Fig. S1-S12, ESI†).

Photophysical properties of the donor acceptor systems

The UV-Visible absorption and fluorescence spectra of the dyads **1** and **2** have been studied in toluene solution and neat

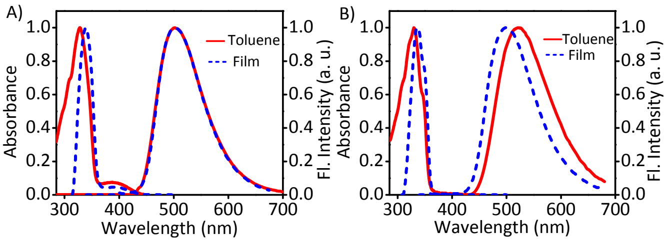

Fig. 1 Normalized absorption and fluorescence spectra at 298 K of the dyads (10 µM each), A) dyad **1** and B) dyad **2**.

View Article Online
DOI: 10.1039/C7NJ04386D

Table 1 Summary of the photophysical properties of the dyads **1** and **2** in toluene solution and film state.[a]

Dyad	λ_{abs}[b] nm	ε_{max}[b] $M^{-1}\,cm^{-1}$ x 10^4	λ_{ems}[b],nm (Φ_f)[b]	λ_{abs}[c] nm	λ_{ems}[c] , nm (Φ_f) [c]	τ[b] (ns)	<τ>[b] (ns)	Kr[b] ($10^7\,S^{-1}$)	Knr[b] ($10^7\,S^{-1}$)
1	390, 328	0.39, 5.17	502 (0.18±0.03)	395, 338	500 (0.25±0.02)	τ_1= 2.03 (3.67%) τ_2= 7.53 (96.33%)	6.85	2.63	11.97
2	345, 330	3.29, 5.50	522 (0.03)	348, 338	500 (0.03)	τ_1= 3.14 (4.42%) τ_2= 13.69 (95.58%)	11.92	0.252	8.14

[a] Average of more than three independent experiments, [b] measured for toluene and [c] measured for spin cast film. λ_{abs}: absorption wavelength, ε_{max}: molar extinction coefficient, λ_{ems}: emission wave length, Φ_f: absolute quantum yield, τ: fluorescent lifetime, <τ>: average fluorescent lifetime, Kr: radiative decay and Knr: non radiative decay.

films, obtained by spin coating of a solution in toluene on the quartz plates (Fig. 1). A broad absorption peak at around 390 nm observed for the dyad **1** can be assigned to the charge transfer transition from the electron donating phenoxazine group to the electron accepting oxadiazole moiety.[29] Interestingly, we observed negligible absorption at 390 nm and formation of a new broad band having absorption in the region from 345 to 380 nm, as the position of the phenoxazine moiety changed from the para-position (dyad **1**) to the meta-position (dyad **2**). These observations can be attributed to the decreasing conjugation between the donor and acceptor subunits in case of the dyad **2** owing to its meta-linkage, which is in agreement with the literature reports.[30]

When the emission properties were investigated in toluene, we observed green fluorescence having λ_{max} at 502 and 522 nm (excited at 330 nm) for the dyads **1** and **2**, respectively. Similar to the solution, the thin film of **1** showed a broad and less intense absorption peak at around 390 nm and an intense peak at 338 nm. Similar observations made with the dyad **2** and which showed peaks at 348 nm and 337 nm. The emission maximum of the films of **1** and **2** were observed at 500 nm (excited at 330 nm). In Fig. 1, the higher Stokes shift of the dyads **1** and **2** is attributed to the charge transfer excited state. The emission maxima of the dyad **1** matched with that observed for the toluene solution. This indicates that the dielectric constant of the film of **1** is close to that of toluene solution. In addition, we have noticed a substantial decrease in the fluorescence quantum yields, when the position of the donor moiety changed from the para- (dyad **1**, Φ_f = 0.18) to meta- position (dyad **2**, Φ_f = 0.03). The calculated CIE coordinates of the dyads **1** and **2** were found to be (0.25, 0.46) and (0.26, 0.48) in toluene and (0.28, 0.53) and (0.26, 0.50) in the film state, respectively, which are characteristic of pure green emission (Fig. S13, ESI†).[31]

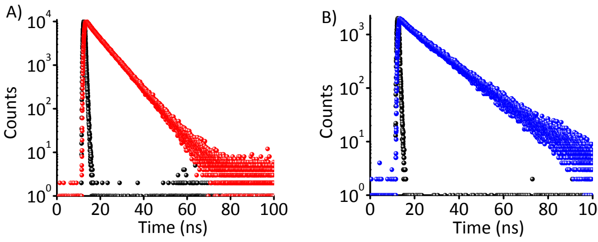

Fig. 2 Fluorescence decay curves of A) dyad **1** and B) dyad **2** in toluene.

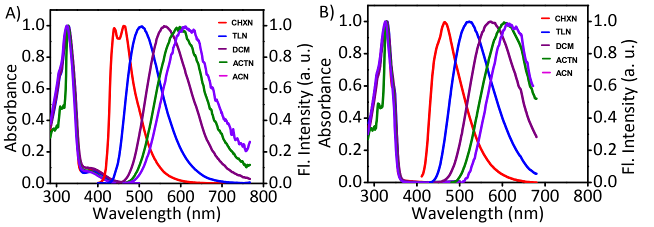

Fig. 3 Absorption and fluorescence spectra of the A) dyad **1** and B) dyad **2** in different solvent (10 μM each).

The fluorescence lifetimes of the dyads **1** and **2** were measured in toluene and the results are summarized in Table 1 and Fig. 2. Both the dyads exhibited biexponential decay with a short lived minor component and a comparatively long-lived major component (τ_1 = 2.03 ns (3.67%) and τ_2 = 7.53 ns (96.33%) for **1**; τ_1 = 3.14 ns (4.42%) and τ_2 = 13.69 (95.58%) for **2**). The observed biexponential decay can be attributed to the presence of different conformers due to the existence of restricted rotation.[32] By using the fluorescence quantum yield (Φ_f) and averaged lifetimes (<τ>), the rate constants of radiative (kr) and non-radiative (knr) decay of the dyads were calculated according to Equations (1) and (2).[33]

$$K_r = \frac{\Phi_f}{\tau} \quad \ldots\ldots\ldots 1$$

$$K_{nr} = \frac{(1-\Phi_f)}{\tau} \quad \ldots\ldots\ldots 2$$

The absorption and emission spectra of dyads **1** and **2** were recorded in various solvents of differing polarity (Fig. 3). The negligible change in the absorption spectra with increasing solvent polarity (nonpolar cyclohexane to polar acetonitrile) is attributed to a small difference between the dipole moments of Franck–Condon excited and ground states. As the polarity of the solvent increased, we observed the broadening of the spectrum with a gradual increase in red shift. From the non-polar cyclohexane to polar acetonitrile, we observed a red shift of *ca.* 155 nm (5380 cm^{-1}) and 160 nm (5500 cm^{-1}) for the dyads **1** and **2**, respectively (Tables S1 and S2, ESI†). These observations indicate that the solvent-solute interactions found to stabilize the intramolecular charge transfer excited states, yielding a dipole moment that is larger than that in the ground state.

View Article Online
DOI: 10.1039/C7NJ04386D

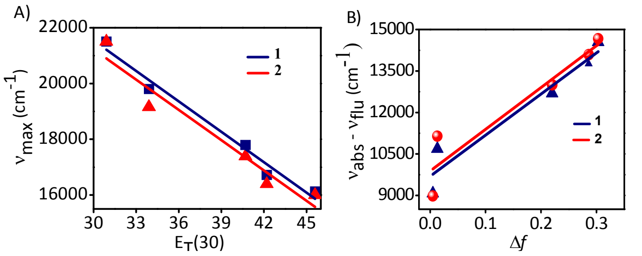

Fig. 4 A) Plot of the emission maximum in different solvents *vs* solvent polarity parameter $E_T(30)$ and B) plot of Stokes shift against the solvent polarity (Δf). From the left, cyclohexane, toluene, dichloromethane, acetone and acetonitrile solutions. The solid lines are the least-squares fit.

The emission maxima (ν_{max}, in wave number) are plotted against the solvent polarity parameter $E_T(30)$ as shown in Fig. 4A. These systems exhibited a positive solvatochromism with the emission maxima depending approximately linearly on the solvent polarity.

$$\nu_{abs} - \nu_{flu} = \frac{1}{4\pi\varepsilon_0}\frac{2\Delta\mu^2}{hca^3}\Delta f + \text{constant} \ldots\ldots\ldots 3$$

Furthermore, the solvent polarity effect was analyzed in terms of the changes in the dipole moment (Δμ) between the ground (S_0) and excited states (S_1) using a Lippert–Mataga plot.[34] From the changes in Stokes shift in different solvents, the change in the dipole moment was calculated using the equation (3), wherein, 'ν_{abs}' and 'ν_{fluo}' are the absorption and fluorescence of the dyads **1** and **2** in wave numbers, respectively, 'ε_0' is the vacuum permittivity, 'h' is the Plank's constant, 'c' is the speed of light and 'a' is the Onsager cavity radius, which was *ca.* 6.36 and 6.31 A^0 for the dyads **1** and **2**, respectively as determined from DFT calculations using Gaussian 09**.** The term Δf, known as the solvent polarity parameter was obtained by the equation ((ε-1)/ (2ε+1)) – ((n^2-1)/ ($2n^2$+1)), wherein ε is the dielectric constant and n is the refractive index of the solvent. The Stokes shift for emissions changed linearly with Δf as shown in Fig. 4B. Using the slope value of *ca.* 14874 and 15098 cm^{-1} for the dyads **1** and **2**, respectively, and equation (1), we have estimated the dipole moment change (Δμ), which is found to be *ca.* 19.51 and 19.42 D for the dyads **1** and **2**, respectively. The calculated dipole moment for the ground states obtained from DFT calculations are *ca.* 4.68 and 1.91 D while the dipole moment of the charge transfer states obtained by the solvatochromic method are *ca.* 24.19 and 21.33 D for the dyads **1** and **2,** respectively. These results clearly indicate that the high dipole moment of the charge transfer states is responsible for the solvent polarity dependent red shifted emission observed for the dyads, which in agreement with the literature reported examples.[35]

Electrochemical, thermal and morphological analysis

Cyclic voltammetric measurements were performed for dyads **1** and **2** in dry DCM with 0.1 M tetrabutylammonium hexafluorophosphate (Bu_4NPF_6) as the supporting electrolyte, under argon atmosphere. The dyads showed reversible oxidation waves due to the presence of electron donating phenoxazine group. The oxidation potentials *vs* Ag/Ag$^+$ were measured to be *ca.* 0.82 and 0.81 V for the dyads **1** and **2**, respectively (Fig. 5A). The redox potential of Fc/Fc$^+$ (standard value = 4.8 eV with respect to vacuum) was observed at 0.43 V. Based on this, the HOMO energy levels of molecules were estimated using the equation E^{HOMO} = – E^{ox} – 4.37 eV, while the LUMO energy levels were obtained from the band gap energies (estimated from the onset wavelengths of the UV absorptions).[36] The thermal properties of the compounds were investigated by using Thermogravimetric analysis (TGA) (Fig. 5B) and both these dyads were found to be thermally quite stable. The decomposition temperature (T_d), defined as the temperature at which 5% mass loss occurs of the dyads **1** and **2** were found to be *ca.* 425 and 412 °C and the melting points of the systems are *ca.* 119 and 134 °C, respectively. The film forming properties were investigated through atomic force microscopy (AFM).[37] The AFM images of solution processed films revealed smooth and homogeneous film morphologies with very small values of root mean square (RMS) roughness of *ca.* 0.39 and 0.40 nm for the dyads **1** and **2,** respectively (Fig. 5C). These results demonstrate that both the dyad molecules have a good film forming ability by a solution process.

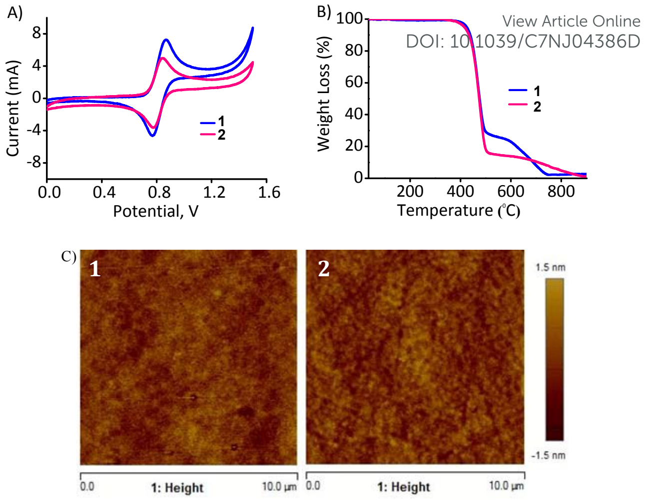

Fig. 5 A) Cyclic voltammograms recorded for the dyads in dry dichloromethane (1 mM solutions; scan rate, 100 mV/s) and B) Thermogram of the dyads **1** and **2** in N_2 atmosphre at a heating rate of 10 ^{0}C/min; C) AFM images of the spin coated films of dyads **1** and **2** on ITO substrate.

Theoretical calculations

The geometry of the dyads **1** and **2** were optimized using B3LYP/6-311G (d,p) level density functional theory. In the cases of **1** and **2**, the dihedral angle (θ_d) between the donor moiety (phenoxazine unit) and the adjacent phenyl ring is *ca.*

Table 2 Physical and electrochemical data of the dyads **1** and **2**.

Dyads	HOMO/LUMO /ΔE (eV)^a	HOMO/LUMO /ΔE (eV)^b	θ_d^{b} (°C)	Mp/T_d (°C)
1	5.19/2.27/2.92	5.07/2.17/2.9	88.5	119 / 425
2	5.18/1.74 /3.44	5.08/2.14/2.94	89.2	134 / 412

[a] Experimentally determined; [b]Theoretically calculated.

View Article Online
DOI: 10.1039/C7NJ04386D

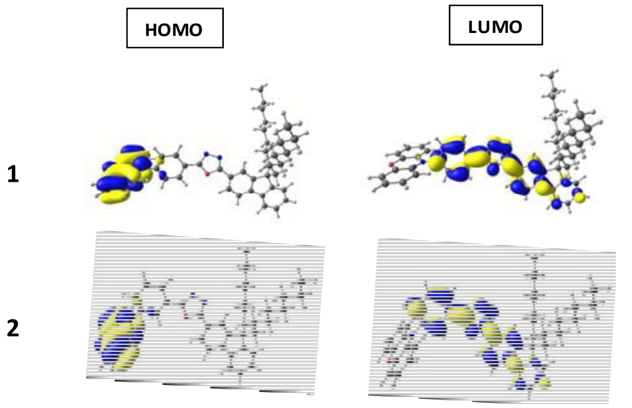

Fig. 6 HOMO and LUMO of the dyads **1** and **2** calculated at the B3LYP/6-311G (d,p) level

88.5° and 89.2°, respectively. In any of the molecules, a planar orientation of the donor moiety with respect to the plane of the N-connected phenyl ring is impossible as this would lead to close proximity between C-H bonds of the donor moiety and N- connected phenyl ring. In other words, the non-bonded H...H interactions (steric repulsion) is responsible for the twisted configurations observed (Fig. S14, ESI†). In Fig. 6, the HOMO and LUMO of the dyads **1** and **2** are depicted using isosurface value 0.03. Since the phenoxazine moiety is nearly orthogonal to the N- connected phenyl ring, the HOMO is seen exclusively centered on the donor moiety. The HOMO/LUMO values obtained are 5.07/2.9 eV for the dyad **1** and 5.08 /2.94 eV for the dyad **2** (Table 2).

Device fabrication

To study the utility of the dyads **1** and **2** in device applications, un-doped OLEDs were fabricated with device configuration having indium tin oxide (ITO) (120 nm)/ Poly(3,4-ethylene-dioxythiophene)-poly(styrenesulfonate) (PEDOT:PSS) (40 nm)/ **1** or **2** (50 nm)/ 1,3,5-tris(N-phenylbenzimidazol-2-yl)-benzene (TPBi) (40 nm)/ LiF(1 nm)/ Al (100 nm). Here, ITO was used as a transparent anode, PEDOT:PSS as the hole-injection layer (HIL), TPBi as the hole-blocking layer (HBL), LiF (lithium fluoride) as the electron-injecting layer (EIL) and Al (aluminium) as cathode.

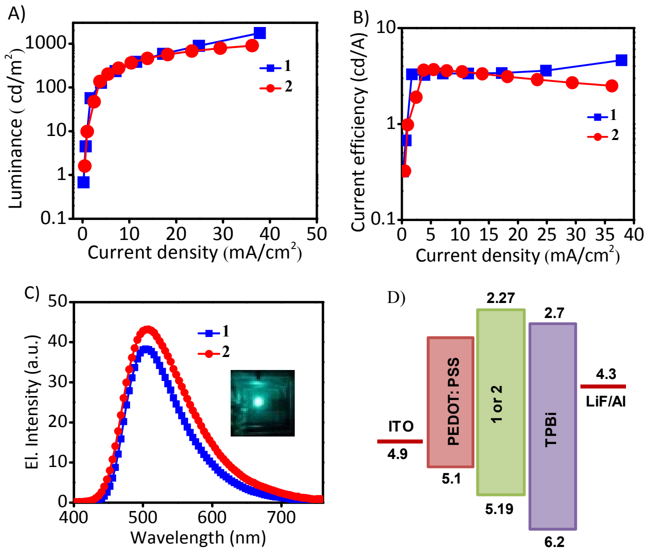

Fig. 7 A-C) Device characteristics and D) energy level diagram of the un-doped solution processed OLEDs fabricated using the dyads **1** and **2**. Inset shows the photograph of electroluminescence from the fabricated device using the dyad **1**.

The dyads **1** and **2** showed green electroluminescence (EL) having λ_{max} at 504 nm and 505 nm with CIE coordinates of (0.26, 0.49) and (0.27, 0.47), respectively (Fig. S15, ESI†). The EL spectra of devices were similar to the photoluminescence spectra of the spin coated films. Good diode behavior was observed for the fabricated devices, which are shown in Fig. S15B, ESI†. The turn on voltage (V_{onset}) for these systems is found to be *ca.* 5.5-6 V. The dyad **1** showed a highest luminance of *ca.* 1751 cd/m^2 with a current efficiency of *ca.* 4.63 cd/A. In the case of dyad **2** having phenoxazine in meta position, comparatively a lower luminance of 903.5 cd/m^2 with current efficiency of 3.65 cd/A was observed. This observation is in accordance with the observed higher fluorescence quantum yield of the dyad **1**. The current density – luminance, current density - current efficiency and voltage - power efficiency characteristics of OLEDs with dyads **1** and **2** are shown in Fig. 7 and the values are tabulated in Table 3. It is very interesting to see that our devices do not suffer from efficiency roll-off, which is a major problem faced by OLEDs.

The efficiency of the devices that incorporated the dyad **1** was found to be superior when compared to that of the dyad **2** derivatives and which confirms the importance of the nature and position of the substitution in these dyads. A comparative performance table of related D-A systems and their device parameters are summarised in Table S3 of the supporting information.

Table 3 Electroluminescence data of the dyads **1** and **2** in OLED device

Dyads	V_{onset} (V)	λ_{ems}	CIE coordinates	L_{max} (cd/m^2)	η_c (cd/A)	η_p (lm/W)
1	5.98	504	(0.26, 0.49)	1751.0	4.63	1.26
2	5.52	505	0.27, 0.47)	903.5	3.65	1.04

V_{onset}: turn-on voltage; λ_{ems}: emission wavelength; L_{max}: maximum luminance; η_c: maximum current efficiency measured; η_p: maximum power efficiency measured. Applied voltage in each case was in the range 11-11.5 V.

Conclusions

In conclusion, we synthesized new green fluorescent organic D-π-A dyads **1** and **2** and have studied their photphysical, thermal, electrochemical and morphological properties as well as their use in OLEDs. Both the dyads **1** and **2** showed favorable photophysical properties and excellent thermal stability, solution processability and film morphologies. The solution processed un-doped green OLEDs fabricated based on these dyads showed CIE coordinates of (0.26, 0.49) and (0.27, 0.47) for the dyads **1** and **2**, respectively, as green emitters with a luminance of *ca.* 1751 cd/m^2 for the dyad **1** and thereby demonstrating its potential use in various optoelectronic applications including in OLEDs.

DOI: 10.1039/C7NJ04336D

Experimental

The melting points were determined on a Mel-Temp II melting point apparatus. The electronic absorption spectra were recorded on a Shimadzu UV-3101 or 2401 PC UV-VIS-NIR scanning spectrophotometer. The fluorescence spectra were recorded on a SPEX-Fluorolog F112X spectrofluorimeter. Film-state photoluminescence was measured using the front face emission scan mode on a SPEX Fluorolog F112X spectrofluorimeter.[38] Measurements of solution state and film-state fluorescence quantum efficiency were carried out using a calibrated integrating sphere in a SPEX Fluorolog spectrofluorimeter. A Xenon-arc lamp was used to excite the film samples placed in the sphere, with 330 nm as the excitation wavelength. This experimental setup and the integrating sphere system calibrated using the solid state fluorescence quantum yield of the standard sodium salicilate (white powder) was determined to be 60 ± 10%, which is consistent with previously reported values.[39] Fluorescence lifetimes were measured using an IBH (Fluoro Cube) time correlated picosecond single photon counting (TCSPC) system.

The CIE, Commission International de l'Eclairage (International Commission on Illumination), chromaticity coordinates (1931) (x, y) were calculated using HORIBA Jobin Yvon Color Calculator provided with integrating sphere. Thermal stability measurements were performed at a heating rate of 10°C/min in a nitrogen atmosphere using Shimadzu, DTG-60 equipment. Cyclic voltammetry is done by CV-50w electro analyzer in DCM using Pt wire as auxiliary electrode, glassy carbon as working electrode. The potential were referenced to the standard Ag/AgCl electrode and ferrocene was used as external standard. ^{1}H NMR was recorded on a 500 MHz Bruker advanced DPX spectrometer. Mass spectra were recorded either on a JEOL AX503 (HRMS) or Shimadzu Biotech Axima CFR plus instrument. The AFM studies were carried out Bruker nanoscope V multimode 8 AFM. All experiments were carried out at room temperature (25±1 °C), unless otherwise mentioned.

The geometry of the dyads **1** and **2** were optimized with B3LYP/6-311G (d,p) level density functional theory[40] in conjunction with polarized continuum model (PCM)[41] solvation method (selected solvent is toluene) as implemented in Gaussian 09 package.[42] Vibrational frequency calculations were carried out on **1** and **2** at the same level of theory and verified them as true minima on the potential energy surface (number of imaginary frequency = 0). The electroluminescent properties of the molecules were studied by fabricating undoped OLEDs by solution processing. The ETL and cathode were deposited using thermal evaporation at a base pressure of 10^{-8} Torr. Patterned ITO coated glass substrates with a sheet resistance of 10 Ω/sq were used as anodes, which were cleaned with detergent, chloroform, isopropanol and de-ionized water and UV–Ozone treated. On the ITO substrate, the HIL, emitting layer, ETL, EIL, and cathode were deposited sequentially without exposing to atmosphere inside glove box. The deposition rate of TPBi and Al was maintained at 2 Å s^{-1}, whereas the deposition rates of LiF were 0.1 Å s^{-1}. The deposition rate and thickness of the deposited layers were controlled in situ by a quartz crystal thickness monitor. The cathode was deposited on the top of the structure through a shadow mask. The devices were encapsulated using UV curable epoxy inside the glove box. The EL spectra, J–V characteristics of the devices were measured using a spectrophotometer and a source meter interfaced to a computer. All of the measurements were carried out at room temperature.

Synthesis of the compound

Bromo-9H-fluorene (b). To a stirred solution of fluorene (a) (1 g, 6.02 mmol) and HBr 48% (1 mL, 6.02 mmol) in CH_2Cl_2-H_2O (9:1, 20 mL) was slowly added H_2O_2 30% (0.68 mL, 6.02 mmol) over a period of 15 min at 10-15 °C. The reaction was left at room temperature for 15 h whilst monitoring its progress by TLC. After the reaction, solvent was removed under reduced pressure and the crude product was taken in the ethyl acetate and washed with water, brine and dried over anhydrous Na_2SO_4. The pure product isolated by silica gel column chromatography. (1.08 g, 73%), mp 112-114 °C; ^{1}H NMR (500 MHz, $CDCl_3$, TMS) δ 3.86 (s, 2H), 7.31 (m, 1H), 7.36 (t, 1H, J = 7 Hz), 7.47 (m, 1H), 7.52 (d, 1H, J = 7.5 Hz), 7.62 (d, 1H, J = 8 Hz), 7.65 (s, 1H), 7.74 (d, 1H, J = 7.5 Hz).

2-Bromo-9,9-dioctyl-9H-fluorene (c). A solution of 2-bromofluorene (1g, 4.08 mmol) in DMSO (15 mL) was degassed by purging with argon for 30 min, and then benzyl triethyl ammonium chloride and aq. NaOH (0.818 g, 20.4 mmol) were added. After 10 minute the reaction mixture turned to red, octyl bromide (2.85 mL) was added and the reaction mixture was heated to 80 °C for 4 h. The reaction mixture subsequently cooled to room temperature, poured in to DCM and washed with H_2O. The organic layer separated and dried over anhydrous Na_2SO_4 and solvent removed by vacuum evaporator. The pure compound isolated by silica gel column chromatography. (1.7 g, 89%); ^{1}H NMR (500 MHz, $CDCl_3$, TMS) δ 0.59 (s, 4H), 0.81 (t, 6H, J = 7 Hz), 1.08 (m, 8H), 1.12 (m, 8H), 1.19 (m, 4H), 1.93 (m, 4H), 7.32 (d, 3H, J = 9.5 Hz), 7.44 (d, 2H, J = 8 Hz), 7.55 (d, 1H, J = 8 Hz), 7.65 (d, 1H, J = 4.5 Hz).

9,9-Dioctyl-9H-fluorene-2-carbonitrile (d). 2-Bromo-9,9-dioctyl-9H-fluorene (1g, 2.13 mmol) dissolved in NMP (15 mL) and then added CuCN (0.572 g, 6.39 mmol) and refluxed overnight. After completing the reaction added 1 g of $FeCl_3$ in 10 mL of 10% HCl and stirred for 0.5 h at 120 °C. Then the reaction mixture cooled to room temperature and extracted twice with toluene. The combined extract washed with 6N HCl, H_2O, and then by 10% NaOH solution. The organic part dried and performed column chromatography. (0.625 g, 70%); ^{1}H NMR (500 MHz, $CDCl_3$, TMS) δ 0.56 (t, 4H, J = 7 Hz), 0.81 (t, 6H, J = 7 Hz), 1.08 (m, 8H), 1.13 (m, 8H), 1.20 (m, 4H), 1.96 (m, 4H), 7.38 (m, 3H), 7.62 (d, 1H, J = 9.5 Hz), 7.65 (d, 1H, J = 8.5 Hz), 7.75 (t, 2H, J = 8.5 Hz); ESI-MS: Calcd for $C_{30}H_{41}N$, 415.32; Found, 416.33 (M^+).

5-(9,9-Dioctyl-9H-fluoren-2-yl)-2H-tetrazole (e). To a mixture of 9,9-Dioctyl-9H-fluorene-2-carbonitrile (1 g, 2.4 mmol) and NaN_3 (0.312 g, 4.8 mmol) in dry toluene (15 mL) was added Bu_3SnCl (1.3 mL, 4.8 mmol). Then stirred and refluxed for 24 h.

After cooling to room temperature the above solution poured to DCM and extracted with water and the organic layer was dried and carried out column chromatography. (0.75 g, 70%), ^{1}H NMR (500 MHz, $CDCl_3$, TMS) δ 0.56 (t, 4H, J = 7 Hz), 0.81 (t, 6H, J = 7 Hz), 1.08 (m, 8H), 1.13 (m, 8H), 1.20 (m, 4H), 1.96 (m, 4H), 7.37 (s, 3H), 7.74 (t, 1H, J = 4.5 Hz), 7.87 (d, 1H, J = 8 Hz), 8.16 (d, 1H, J = 8Hz), 8.23 (s, 1H) ESI-MS: Calcd for $C_{30}H_{42}N_4$, 458.34; Found, 459.34 (M^+).

2-(4-Bromophenyl)-5-(9,9-dioctyl-9H-fluoren-2-yl)-1,3,4-oxadiazol (p-FOArBr). A solution of *p*-Bromobenzoyl chloride (0.717 g, 3.27 mmol) was added drop wise to a solution of tetrazol (1 g, 2.18 mmol) in pyridine (20 mL) and refluxed for 2 h under argon. The reaction mixture is then cooled to room temperature prior to being poured in to methanol with stirring to precipitate the product. (1 g, 75%), mp = 72-74 °C, ^{1}H NMR (500 MHz, $CDCl_3$, TMS) δ 0.60 (m, 4H), 0.78 (t, 6H, J = 7 Hz), 1.08 (m, 16H), 1.15 (m, 4H), 2.03 (m, 4H), 7.38 (t, 3H, J = 2.5 Hz), 7.70 (m, 2H), 7.77 (m, 1H), 7.84 (t, 1H, J = 4.5 Hz), 8.06 (m, 2H, 8.09 (t, 2H, J = 2.5 Hz). ^{13}C NMR (125 MHz, $CDCl_3$) 165.50, 163.72, 151.69, 151.44, 145.04, 139.81, 132.44, 128.36, 127.08, 126.33, 126.08, 123.01, 121.97, 121.33, 120.48, 120.23, 55.50, 40.28, 31.74, 29.94, 29.21, 29.16, 23.76, 22.56, 14.03. ESI-MS: Calcd for $C_{37}H_{45}BrN_2$, 612.27; Found, 613.27 (M^+).

2-(3-Bromophenyl)-5-(9,9-dioctyl-9H-fluoren-2-yl)-1,3,4-oxadiazole (m-FOArBr). A solution of m-Bromobenzoyl chloride (0.717 g, 3.27 mmol) was added dropwise to a solution of tetrazol (1 g, 2.18 mmol) in pyridine (20 mL) and refluxed for 2 h under argon. Then cooled to room temperature prior to being poured in to methanol with stirring to precipitate the product (1 g, 69%), mp = 77-79 °C, ^{1}H NMR (500 MHz, $CDCl_3$, TMS) δ 0.62 (t, 4H, J = 7 Hz), 0.80 (t, 6H, J = 7 Hz), 1.08 (m, 16H), 1.18 (m, 4H), 2.08 (m, 4H), 7.38 (d, 3H, J= 9.5 Hz), 7.43 (t, 1H, J = 8 Hz), 7.70 (d, 1H, J = 8 Hz), 7.77 (t, 1H, J = 4 Hz), 7.85 (d, 1H, J = 8 Hz), 8.12 (t, 3H, J = 9 Hz), 8.33 (s, 1H). ^{13}C NMR (125 MHz, $CDCl_3$) 165.63, 163. 12, 151.71, 151.44, 145.11, 139.79, 134.60, 130.67, 129.72, 128.40, 127.08, 126.14, 125.90, 125.52, 123.13, 123.05, 121.85, 121.36, 120.50, 120.25, 55.51, 40.28, 31.74, 29.94, 29.21, 29.17, 23.76, 22.56, 14.04. ESI-MS: Calcd for $C_{37}H_{45}BrN_2$, 612.27; Found, 613.27 (M^+).

10-(4-(5-(9,9-Dioctyl-9H-fluoren-2-yl)-1,3,4-oxadiazol-2-yl)phenyl)-10H-phenoxazine (1). A mixture of *p*-FOArBr (1 g, 1.633mmol), phenoxazine (0.448 g, 2.45 mmol), Cs_2CO_3 (1.596 g, 4.899 mmol), $Pd(OAc)_2$ (37 mg, 0.1633 mmol) and $p(tBu)_3$ (99 mg, 0.49 mmol) in toluene (30 mL) was heated at 40 °C for 2 h and then the reaction mixture heated at 110 °C for 24 h. After the mixture was cooled to room temperature water and chloroform added, organic layer was separated and dried under reduced pressure. Column chromatography was carried out over silica gel using a 5% mixture of ethyl acetate and hexane. (0.94 g, 80%), ^{1}H NMR (500 MHz, $CDCl_3$, TMS) δ 0.62 (s, 4H), 0.79 (t, 6H, J = 7 Hz), 1.09 (m, 16H), 1.17 (m, 4H), 2.05 (m, 4H), 6.01(d, 2H, J = 7.5 Hz), 6.63 (m, 2H), 6.71 (m, 4H), 7.39 (d, 3H, J = 2 Hz), 7.57 (d, 2H, J = 8.5 Hz), 7.78(m, 1H), 7.86(d, 1H, J = 8 Hz), 8.14(t, 2H, J = 3.5 Hz), 8.42 (d, 2H, J = 8.5 Hz). ^{13}C NMR (125 MHz, $CDCl_3$) 165.63, 163.71, 151.73, 151.44, 145.09, 144.00, 142.26, 139.80, 133.79, 131.77, 129.70, 128.41, 127.11, 126.11, 124.08, 123.35, 123.08, 121.97, 121.86, 121.35, 120.51, 120.28, 115.75, 113.28, 55.51, 40.29, 31.76, 29.96, 29.22, 29.19, 23.78, 22.57, 14.06. ESI-MS: Calcd for $C_{49}H_{53}N_3O_2$, 715.41; Found 716.42 (M+).

10-(3-(5-(9,9-Dioctyl-9H-fluoren-2-yl)-1,3,4-oxadiazol-2-yl)phenyl)-10H-phenoxazine (2). A mixture of *m*-FOArBr (1 g, 1.633 mmol), phenoxazine (0.448 g, 2.45 mmol), Cs_2CO_3 (1.596 g, 4.899 mmol), $Pd(OAc)_2$ (37 mg, 0.1633 mmol) and $p(t\text{-}Bu)_3$ (99 mg, 0.49 mmol) in toluene (30 mL) was heated at 40 °C for 2 h and then the reaction mixture heated at 110 °C for 24 h. After the mixture was cooled to room temperature water and chloroform added, organic layer was separated and dried under reduced pressure. Column chromatography was carried out over silica gel using a 5% mixture of ethyl acetate and hexane. (0.88 g, 75%), ^{1}H NMR (500 MHz, $CDCl_3$, TMS) δ 0.58 (t, 4H, J = 6.5 Hz) 0.78 (t, 6H, J = 7 Hz), 1.06 (m, 16H), 1.17 (m, 4H), 2.05 (m, 4H), 5.97(m, 2H), 6.63 (m, 2H), 6.69 (m, 2H), 6.74 (m, 2H), 7.37 (t, 3H, J = 2.5 Hz), 7.58 (m, 1H), 7.76(m, 1H), 7.81(m, 1H), 8.13 (m, 3H), 8.35 (m, 1H). ^{13}C NMR (125 MHz, $CDCl_3$) 165.66, 163. 46, 151.71, 151.44, 145.08, 143.95, 140.00, 139.82,134.47, 133.97, 132.10, 129.50, 128.37, 127.31, 127.12, 127.06, 126.19, 123.38,123.05, 121.87, 121.80, 121.33, 120.50, 120.25, 115.71, 113.26, 55.54, 40.26, 31.73, 29.92, 29.22, 23.76, 22.56, 14.04. ESI-MS: Calcd for $C_{49}H_{53}N_3O_2$, 715.42; Found 716.42 (M^+).

Conflicts of interest

There are no conflicts to declare.

Acknowledgements

We acknowledge the financial support from CSIR-TAPSUN program (NWP0054) and DST, Government of India. ST and AS thank UGC for research fellowship and J.J. thanks DST for the Ramanujan Fellowship. We thank Dr. C. H. Suresh and Ms. Della Therese Davis for their help in the theoretical calculations. This work is contribution No. PPG–370 from CSIR-NIIST, Thiruvananthapuram.

Notes and references

1 M. A. Baldo, S. Lamansky, P. E. Burrows, M. E. Thompson, and S. R. Forrest, *Appl. Phys. Lett.,* 1999, **75**, 4; G. M. Farinola and R. Ragni, *Chem. Soc. Rev.*, 2011, **40**, 3467; R. K. Konidena, K. R. Thomas, S. Kumar, Y. C. Wang, C. J. Li and J. H. Jou, *J. org. chem.*, 2015, **80**, 5812.
2 C. W. Tang and S. A. VanSlyke, *Appl. Phys. Lett.,* 1987, **51**, 913.
3 Q. Tong, S. Lai, M. Chan, Y. Zhou, H. Kwong, C. Lee and S. Lee, *Chem. Mater.*, 2008, **20**, 6310.
4 C. Adachi, T. Tsutsui and S. Saito, *Appl. Phys. Lett.*, 1990, **57**, 531; M. Tsai, H. Lin, H. Su, T. Ke, C Wu, F. Fang, Y. Liao, K. Wong and C. Wu, *Adv. Mater.,* 2006, **18**, 1216; M. K. Kim, J. Kwon, T. Kwon, J. Hong, *New J. Chem.*, 2010, **34**, 1317.
5 J. Jou, S. Kumar, A. Agrawal, T. Lia and S. Sahoo, *J. Mater. Chem. C*, 2015, **3**, 2974.

6 J. Jou, S. Kumar, A. Agrawal, T. Lia and S. Sahoo, *J. Mater. Chem. C*, 2015, **3**, 2974.

7 H. Jiang, *Macromol. Rapid Commun*., 2010, **31**, 2007.

8 X. H. Zhu, J. Peng, Y. Cao and J. Roncali, *Chem. Soc. rev.*, 2011, **40**, 3509.

9 F. Huang, Y. J. Cheng, Y. Zhang, M. S. Liu and A. K. Y. Jen, *J. Mater. Chem.*, 2008, **18**, 4495; L. Yao, S. Xue, Q. Wang, W. Dong, W. Yang, H. Wu, M. Zhang, B. Yang, Y. Ma, *Chem. Eur. J.*, 2012, **18**, 2707.

10 Y. Shirota, M. Kinoshita,T. Noda, K. Okumoto, and T. Ohara., *J. Am. Chem. Soc.*, 2000, **122**, 11021; Y. Yuan, G. Zhang, F. Lu, Q. Tong, Q. Yang, H. Mo, T. Wai, M. Lo, Z. Guo, C. Wu, and C. Lee, *Chem. Asian J.,* 2013, **8**, 1253.

11 L. Duan, L. Hou, T. Lee, J. Qiao, D. Zhang, G. Dong, L. Wanga and Y. Qiu, *J. Mater. Chem.*, 2010, **20**, 6392.

12 Q. Zhang, *J. Am. Chem. Soc.*, 2014, **136**, 18070.

13 H. Inomata, K. Goushi, T. Masuko, T. Konno, T. Imai, H. Sasabe, J. J. Brown and C. Adachi, *Chem. Mater.*, 2004, **16**, 1285.

14 B. Priyanka, V. Anusha, and K. Bhanuprakash, *J. Phys. Chem. C*, 2015, **119**, 12251.

15 M. Aydemir, G. Haykır, F. Turksoy, S. Gumus, F. B. Dias and A. P. Monkman, *Phys. Chem. Chem. Phys.*, 2015, **17**, 25572.

16 X. Wei, W. Tan, J. Zou, Q. Guo, D. Gao, D. Ma, J. Peng, Y. Cao and X. Zhu, *J. Mater. Chem. C*, 2017, **5**, 2329.

17 S. Gong, Y. Zhao, M. Wang, C. Yang, C. Zhong, J. Qin and D. Ma, *Chem. Asian J.*, 2010, **5**, 2093; D. Karthik, K. R. Justin Thomas, J. Jou, S. Kumar, Y. Chen and Y. Jou, *RSC Adv.,* 2015, **5**, 8727.

18 C. J.Tonzola, A. P. Kulkarni, A. P. Gifford, W. Kaminsky, S. A. Jenekhe, *Adv. Funct. Mater.*, 2007, **17**, 863.

19 B. D. Lindner, Y. Zhang, S. Hofle, N. Berger, C. Teusch, M. Jesper, K. I. Hardcastle, X. Qian, U. Lemmer, A. Colsmann, U. H. F. Bunz and M. Hamburger, *J. Mater. Chem. C*, 2013, **1**, 5718.

20 A. P. Kulkarni, C. J. Tonzola, A. Babel and S. A. Jenekhe, *Chem. Mater.,* 2004, **16**, 4556; A. Paun, N. D. Hadade, C. C. Paraschivescu and M. Matache, *J. Mater. Chem. C*, 2016, **4**, 8596.

21 S. Gong, Y. Chen, X. Zhang, P. Cai, C. Zhong, D. Ma, J. Qin, C. Yang, *J. Mater. Chem.,* 2011, **21**, 11197.

22 N. Prachumrak, S. Pojanasopa, R. Tarsang, S. Namuangruk, S. Jungsuttiwong, T. Keawin, T. Sudyoadsuk and V. Promarak, *New J. Chem.*, 2014, **38**, 3282.

23 N. Kapoor and K. R. J. Thoma, *New J. Chem.*, 2010, **34**, 2739.

24 Y. Park, B. Kim, C. Lee, A. Hyun, S. Jang, J.-H. Lee, Y.-S. Gal, T. H. Kim, K.-S. Kim and J. Park, *J. Phys. Chem. C,* 2011, **115**, 4843.

25 B. Kim, J. Lee, Y. Park, C. Lee, J. W. Park, *J. Nanosci. Nanotechnol.* 2014**, 14**, 6404.

26 J. Lee, K. Shizu, H. Tanaka, H. Nomura,T. Yasudaabc and C. Adachi., *J. Mater. Chem. C*, 2013, **1**, 4599.

27 B. Tsuie, J. L. Reddinger, G. A. Sotzing, J. Soloducho, A. R. Katritzky and J. R. Reynolds, *J. Mater. Chem.,* 1999, **9**, 2189; P. V. Vyas, A. K. Bhatt, G. Ramachandraiah and A. V. Bedekar, *Tet. Lett.,* 2003, **44**, 4085; K. T. Wong, S. Y. Ku, Y. M. Cheng, X. Y. Lin, Y. Y. Hung, S. C. Pu, P. T. Chou, G. H. Lee, and S. M. Peng, *J. Org. Chem.* 2006, **71**, 456; M. A. Reddy, A. Thomas, K. Srinivas, V. J. Rao, K. Bhanuprakash, B. Sridhar,A. Kumar, M. N. Kamalasanan and R.Srivastava, *J. Mater. Chem.,* 2009, **19**, 6172.

28 K. Ono, M. Joho, K. Saito, M. Tomura, Y. Matsushita, S. Naka, H. Okada and H. Onnagawa, *Eur. J. Inorg. Chem.,* 2006, 3676.

29 H. Tanaka, K. Shizu, H. Nakanotani and C. Adachi., *Chem. Mater.,* 2013, **25**, 3766.

30 Y. Tao, Q. Wang, C. Yang, C. Zhong, K. Zhang, J. Qin and D. Ma, *Adv. Funct. Mater.*, 2010, **20**, 304.

31 K. S. Sanju, P. P. Neelakandan and D. Ramaiah, *Chem. Commun.,* 2011, **47**, 1288; K. S. Sanju and D. Ramaiah, *Chem. Commun.,* 2013, **49**, 11626; K. S. Sanju, S. Thurakkal, P. P. Neelakandan, J. Joseph and D. Ramaiah, *Phys. Chem. Chem. Phys.* 2015, **17**, 13495.

32 B. R. Kaafarani, A. a. O. El-Ballouli, R. Trattnig, A. Fonari, S. Sax, B. Wex, C. Risko, R. S. Khnayzer, S. Barlow, D. Patra, T. V. Timofeeva, E. J. W. List, J.-L. Bredas, S. R. Marder, *J. Mater. Chem. C*, 2013, **1**, 1638.

33 M. Viji, A. K. Nair, P. C. Nandajan and D. Ramaiah, *RSC Adv.*, 2014, **4**, 47982; D. Ramaiah, I. Eckert, K. T. Arun, L. Weidenfeller and B. Epe, *Photochem. Photobiol*., 2004, **79**, 99; M. Hariharan, S. C. Karunakaran and D. Ramaiah, *Org. Lett.*, 2007, **9**, 417; K. Jyothish, R. R. Avirah and D. Ramaiah, *Org. Lett.*, 2006, **8**, 111.

34 R. Ishimatsu, S. Matsunami, K. Shizu, C. Adachi, K. Nakano, and T. Imato. *J. Phys. Chem. A,* 2013, **117**, 5607.

35 S. Kim, Y. Cho, A. Lee, H. Son, W. S. Han, D. W. Cho and S. O. Kang, *Phys. Chem. Chem. Phys*., 2017, **19**, 426; R. Chen, G. Zhao, X. Yang, X. Jiang, J. Liu, H. Tian, Y. Gao, X. Liu, K. Han, M. Sun and L. Sun, J. Molec. Struct., 2008, **876**, 102; M. E. Vazquez, J. B. Blanco, B. Imperiali, *J. Am. Chem. Soc.*, 2005, **127**, 1300.

36 E. Ramachandran and R. Dhamodharan, *J. Mater. Chem. C*, 2015, ***3***, 8642; L. D. Chebrolu, S. Thurakkal, H. S. Balaraman, D. Ramaiah, *Sensors and Actuators B*, 2014, **204**, 480. W. Adam, J. Cadet, B. Epe, F. Dall'Acqua, D. Ramaiah and C. R. Saha Möller, *Angew. Chem., Int. Ed. Engl.*, 1995, **34**, 107; J. Joseph, N. V. Eldho and D. Ramaiah, *J. Phys. Chem. B*, 2003, **107**, 4444.

37 V. S. Jisha, K. T. Arun, M. Hariharan, and D. Ramaiah, *J. Am. Chem. Soc.,* 2006, **128**, 6024; E. Kuruvilla, D. Ramaiah *J. Phys. Chem. B,* 2007, **111**, 6549; K. Bhattacharyya, D. Ramaiah, P. K. Das and M. V. George, *J. Phys. Chem*., 1986 **90**, 5984.

38 P. P. Neelakandan and D. Ramaiah, *Angew. Chem. Int. Ed.,* 2008, **47**, 8407; S. C. Karunakaran, P. S. S. Babu, B. Madhuri, B. Marydasan, A. K. Paul, S. A. Nair, K. S. Rao, A. Srinivasan, T. K. Chandrashekar, Ch. M. Rao, M. R. Pillai, and D. Ramaiah, *ACS Chem. Biol.*, 2013, **8**, 127.

39 I. D. Carlos, C. D. M. Donega, R. Q. Albuquerque, S. Alves jr, J. F. S. Menezes, and O. I. Malta, *Molec. Phys.,* 2003, **101**, 1037.

40 R. Krishnan, J. S. Binkley, R. Seeger and J. A. Pople, *J. Chem. Phys.* 1980, **72**, 650; C. Lee, W. Yang and R. G. Parr, *Phys. Rev. B: Condens. Matter,* 1988, **37**, 785; A. D. Becke, *J. Chem. Phys.* 1993, **98**, 5648.

41 S. Miertus, E. Scrocco, Tomasi, *J. Chem. Phys.* 1981, **55**, 117.

42 M. J. Frisch, G. W. Trucks, H. B. Schlegel, G. E. Scuseria, M. A. Robb, J. R. Cheeseman, G. Scalmani, V. Barone, B. Mennucci, G. A. Petersson, H. Nakatsuji, M. Caricato, X. Li, H. P. Hratchian, A. F. Izmaylov, J. Bloino, G. Zheng, J. L. Sonnenberg, M. Hada, M. Ehara, K. Toyota, R. Fukuda, J. Hasegawa, M. Ishida, T. Nakajima, Y. Honda, O. Kitao, H. Nakai, T. Vreven, J. A. Montgomery, Jr, J. E. Peralta, F. Ogliaro, M. Bearpark, J. J. Heyd, E. Brothers, K. N. Kudin, V. N. Staroverov, R. Kobayashi, J. Normand, K. Raghavachari, A. Rendell, J. C. Burant, S. S. Iyengar, J. Tomasi, M. Cossi, N. Rega, N. J. Millam, M. Klene, J. E. Knox, J. B. Cross, V. Bakken, C. Adamo, J. Jaramillo, R. Gomperts, R. E. Stratmann, O. Yazyev, A. J. Austin, R. Cammi, C. Pomelli, J. W. Ochterski, R. L. Martin, K. Morokuma, V. G. Zakrzewski, G. A. Voth, P. Salvador, J. J. Dannenberg, S. Dapprich, A. D. Daniels, Oe. Farkas, J. B. Foresman, J. V. Ortiz, J. Cioslowski and D. J. Fox, Gaussian 09, Revision D.01, Gaussian, Inc., Wallingford, CT, 2009**.**

TABLE OF CONTENTS

View Article Online
DOI: 10.1039/C7NJ04386D

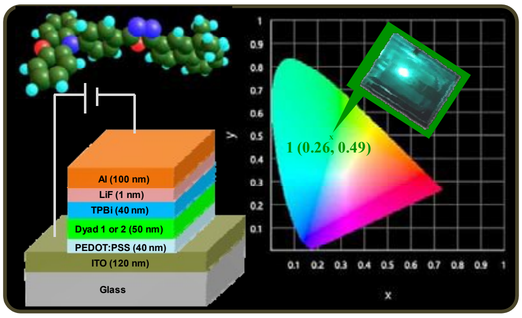

Synthesized solution processable green fluorescent donor-acceptor dyads and investigated their photophysical, electrochemical, and morphological properties for OLED applications.